Floris van Eekert

Determination of paramagnetic Mn(II) concentrations from Bulk Magnetic Susceptibility shifts in NMR spectra

TU Delft

Determination of paramagnetic Mn(II) concentrations from Bulk Magnetic Susceptibility shifts in NMR spectra

By

Floris Michael Theodoor van Eekert

4753674

in partial fulfilment of the requirements for the degree of

Bachelor of Science
in Molecular Science and Technology

at the Delft University of Technology,
to be defended publicly Monday April 12, 2021 at 13:30 PM.

Supervisor:	Prof. Dr. Ir. K. Djanashvili, E. J. van den Heuvel
Thesis committee:	Prof. Dr. Ir. K. Djanashvili, Prof. Dr. Ir. A. G. Denkova

TU Delft

Abstract

The recently discovered negative health effects of Gd(III) complexes based magnetic resonance imaging (MRI) contrast agents have stirred interest into the development of alternatives based on Mn(II) complexes due to its biocompatibility, and hence less health concerns. One important aspect of investigation on contrast agents in general, and Mn(II) complexes in particular, is an accurate determination of their concentrations in solution. Therefore, in this study a known approach of determining the concentration of paramagnetic species in solution, via the Bulk Magnetic Susceptibility (BMS) shift, is applied for Mn(II) and the feasibility of the method is evaluated.

A proof of principle using Gd-DOTP concentrations in the range 0.7 – 6.6 mM Gd(III) to verify the applied BMS method was successfully performed. Subsequently, BMS measurements were performed with Mn-DOTA as well as free Mn(II) and the obtained concentrations were verified with ICP-OES. A good agreement between the two methods was found within the concentration range of 0.4 - 15.1 mM Mn(II) for both Mn-DOTA and free Mn(II). Although, BMS measurements showed slightly higher concentrations than those found by ICP-OES for both Mn-DOTA and free Mn(II). Additionally, the deviations between ICP-OES and BMS were greater for free Mn(II) compared to Mn-DOTA. Experiments for determining the accuracy of the BMS method showed a 2.5% upward systematic error. The random error decreased from 20% for 0.27 mM Mn(II) to almost 0% for 4.0 mM Mn(II) and higher concentrations.

In conclusion, the BMS method proved to be accurate for determining Mn(II) concentrations and has promising prospects for future research into Mn(II) complexes. However, deviations between ICP-OES and BMS measurements need further investigations.

Key words: Bulk Magnetic Susceptibility shift, contrast agent, Mn(II) complexes

List of contents

Abbreviations and acronyms

Abbreviation	Definition
AOS	Average oxidation state
BMS	Bulk Magnetic Susceptibility
CA	Contrast Agent
Cu	Copper
DOTA	1,4,7,10-tetraazacyclododecane-1,4,7,10-tetraacetic acid
DTPA	diethylenetriaminepentaacetic acid
Fe	Iron
GBCA	Gadolinium Based Contrast Agent
Gd	Gadolinium
ICP-OES	Inductively Coupled Plasma – Optical Emission Spectroscopy
Mn	Manganese
MRI	Magnetic Resonance Imaging
NMR	Nuclear Magnetic Resonance
NOTA	2,2′,2”-(1,4,7-triazacyclononane-1,4,7-triyl)triacetic acid
NSF	Nephrogenic Systemic Fibrosis
ppm	Parts per million
TMSP	3-(Trimethylsilyl)propionic-2,2,3,3 – d4 acid sodium salt
T1	Longitudinal relaxation time
T2	Transversal relaxation time
t-BuOH	*tert*-butyl alcohol

1. Introduction

Magnetic resonance imaging (MRI) is a technique used in radiology to provide anatomic images of the human body. In the last decades, this technique has developed to be one of the most important methods used in medical diagnosis. It is based on the same principles as Nuclear Magnetic Resonance (NMR). Here, a nucleus is placed in a magnetic field and a 90° radiofrequency pulse is applied which 'flips' the magnetic moment of the nucleus. After 'flipping' the magnetic moment, the nucleus relaxes back while emitting radiation, which can be measured via the longitudinal (T1) and transversal (T2) relaxation times. The relaxation time for water molecules varies for different organs/tissues in the human body. Based on this principle an image of the human body can be generated. The relaxation times of the organs/tissues can be influenced by the presence of paramagnetic Contrast Agents (CAs). [1-3]

The idea of enhancing contrast of MRI images via CAs was conceived at the beginning of the 1980s.[4] In 1988 the first CA based on Gd(III), chelated by DTPA, was made commercially available, see *figure 1*.[5] Nowadays, CAs are still mostly based on Gd(III) and are applied in 25% of all MRI scans.[6] The success of Gd(III) CAs can be attributed to its strong paramagnetic properties, strong relaxing effect and *in vivo* stability of the complexes it forms with most ligands of interest.[7, 8]

The success of gadolinium based Contrast Agents (GBCAs) was widely accepted until a study in 2006 showed a connection between GBCAs and Nephrogenic Systemic Fibrosis (NSF).[9] The GBCAs are decomposed to highly toxic free Gd(III) over time and accumulated in the kidney tissue.[10] This problem was resolved mostly by using more stable GBCAs and only a few new cases of NSF were reported, since 2009.[11] Nevertheless, recent research demonstrated accumulation of free Gd(III) in the brain tissue of healthy patients, indicating possible new negative health effects from GBCAs that are still under investigation.[12]

Due to the recently discovered side effects of GBCAs, research into new CAs based on other paramagnetic metals has been started. One promising alternative is Mn(II) because of its high spin (S = 5/2) state, resulting in strong paramagnetic properties.[13] In contrast to Gd(III), Mn(II) has no negative health effects on the human body, since Mn(II) is an important biogenic element in several *in vivo* biological pathways. Additionally, Mn(II) is significantly cheaper for CA production than Gd(III).[14]

However, there are also some major downturns in using Mn(II) as a CA compared to Gd(III). Mn(II) is less paramagnetic, has a lower ionic radius and a lower charge compared to Gd(III). Additionally, Mn(II) has a coordination number of six or seven, compared to nine for Gd(III). As a result, it is difficult to find ligands that form stable complexes with Mn(II) and achieve the same strong relaxing effects observed for Gd(III) CAs.[14]

Research has been performed on the thermodynamic and kinetic properties of different Mn(II) ligand combinations as well as their relaxivity enhancing effect. Examples of investigated Mn(II) ligand combinations are: Mn-DOTA *,* see *figure 1,* Mn(II) with macro-cycles containing pyridine moieties, see *figure 1*, and Mn(II) ferrite nanoparticles with water soluble coatings. It was demonstrated that Mn-DOTA and Mn-NOTA complexes are very stable in aqueous solution under the influence of Zn(II). This refutes the in general

accepted assumption that all Mn(II) complexes are kinetically labile.[15] Nevertheless, both Mn-DOTA and Mn-NOTA appear to be unsuitable for use as CA, because the inner sphere of Mn(II) has no free position for a water molecule to coordinate.[15] Furthermore, it was also demonstrated that the addition of a pyridine group in a fifteen membered macro-cycle ring resulted in greater stability of Mn(II) complexes and a higher relaxation rate due to change of coordination number from six to seven.[16] Research regarding Mn(II) ferrite nanoparticles as CA, show feasible relaxation rates.[17-19]

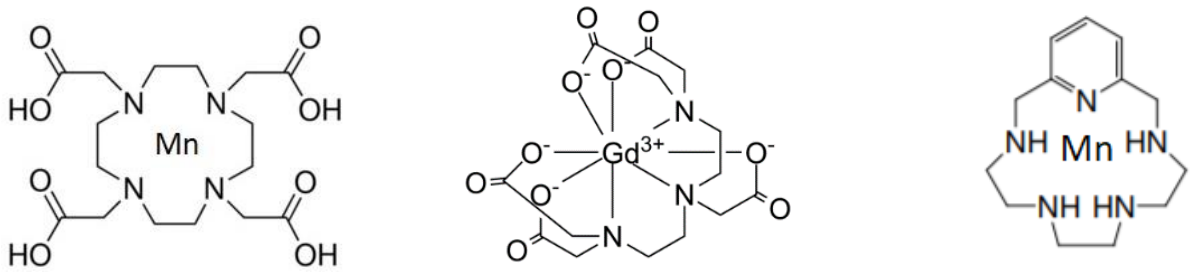

Figure 1: The chemical structure of Mn-DOTA (Left)[20], the chemical structure of Gd-DTPA (Middle), the first commercially used CA.[21] The chemical structure of Mn(II) with a macro-cycle containing pyridine moieties (Right).[16]

Even though Mn(II) seems to be a promising alternative, more elaborate research into the stability and relaxing properties of different potential Mn(II) complexes is required. One aspect of this research is to investigate the concentration of the CA in solution, effectively. The most widely applied method for the concentration determination is via Inductively Coupled Plasma – Optical Emission Spectroscopy (ICP -OES). The principle of ICP-OES is based on detecting the characteristic electro-magnetic radiation of elements as a result of sample ionization in a plasma void. Every element emits its own characteristic wavelengths. The intensity of these wavelengths is translated to a concentration.[22]

ICP-OES has proven to be very accurate. Nevertheless, this method is time consuming, laborious and destroys the used samples. Therefore D. Corsi *et al.*[23] proposed a new method for measuring paramagnetic metal concentrations via the Bulk Magnetic Susceptibility (BMS) shift, which is observed in NMR spectra of solutions containing paramagnetic substances. The method is based on the linear relation between the concentration of lanthanides and the observed BMS. The method proved being able to accurately determine lanthanide concentrations in the desired concentration range.

If the BMS could be adapted for measuring paramagnetic Mn(II) concentrations this could make research into Mn-complexes as a CA more efficient. Therefore, this research project aims at the development of a facile method for the determination of Mn(II) concentration in solution by adopting the similar BMS method known for lanthanides. The reliability of the method will be demonstrated with another quantitative, but more laborious method by ICP-OES.

In this report, the following will be discussed. In **Chapter 2,** an in-depth background of the paramagnetic shift in NMR will be given including a review of the main factors influencing the significance of the paramagnetic shift: the effective magnetic moment and the oxidation state of manganese. This section will also include an overview of the available literature on the paramagnetic shift and a summary the most important aspects of

ICP-OES concerning our research. In **Chapter 3,** the Materials and Methods of the experiments performed will be discussed. In **Chapter 4**, the results and discussions of the experiments will be presented. In **Chapter 5**, Conclusions, and **Chapter 6**, Recommendations, information will be presented that invites to further investigations on the topic.

2. Background

NMR: Paramagnetic Shift

In NMR molecular species are detected by the resonance of nuclei with a specific frequency that is generated by a magnetic field. The magnetic susceptibility of these nuclei can be affected by the presence of a paramagnetic substance present in the same solution. Due to the presence of this paramagnetic substance the resonating frequency of the sample nuclei changes. This results in a chemical shift of the sample peaks on the NMR spectrum, which can be used as the concentration determinant of the paramagnetic substance.[24]

The change of the chemical shift of a nucleus by the influence of a paramagnetic substance can be attributed to three independent contributions: the complex formation shift (Δ_{cf}), the hyperfine shift (Δ_h) and the bulk magnetic shift (Δ_x). The sum of these independent contributions results in *eq. 1* for the total chemical shift induced by a paramagnetic substance.[25]

$$\Delta = \Delta_{cf} + \Delta_h + \Delta_x \quad (1)$$

The complex formation shift results from any chemical interaction of the ligand with the metal-centre during complex formation even if the metal-centre is diamagnetic. Usually, those diamagnetic shifts are small compared to paramagnetic shifts and can therefore be neglected.[26]

The hyperfine shift can be separated in two terms. The first term is the result of unpaired electrons in the resonant nucleus forming a covalent bond with the paramagnetic centre. The second term is the result of dipolar (pseudo-contact) contribution, where the resonant nucleus forms an ion bond with the paramagnetic centre.[27] With those two types of bonds, the paramagnetic centre can influence the shift of the resonant nucleus that binds to the centre. For our reference material, *tert*-butyl alcohol (*t*-BuOH), the hyperfine shift will be neglectable since it will not have a permanent bond with the metal centre.[25]

The BMS is the result of the paramagnetic metal partially aligning with the magnetic field of the NMR, resulting in a shift of the resonance frequency of all the nuclei in the solution. The BMS can be approached with *eq. 2* which forms the basis in the concentration determination of a paramagnetic substance in NMR.[25]

$$\Delta_x = \frac{4\pi CS}{T} \left(\frac{\mu_{eff}}{2.84}\right)^2 \quad (2)$$

The position of the sample to the magnetic field of the NMR is described by *S*, which is assumed to be 1/3 in the case of a cylindrical NMR tube parallel to the main field. *C* is the concentration of the paramagnetic substance in the sample in mol L^{-1}, *T* is the temperature in K and μ_{eff} is the effective magnetic moment, which is a characteristic of the chosen paramagnetic metal. The value of μ_{eff} is determined by a set of fixed

characteristics and in the next section an overview of these fixed characteristics will be given.

Effective magnetic moment

Since the effective magnetic moment of the Mn(II) ion is essential in determining the concentration of Mn(II) out of BMS, it is important to have a thorough understanding of the factors that influence this. Mn(II) is part of the 3d orbital transition metals and the effective magnetic moment therefore depends on two main factors: the spin angular momentum and the orbital angular momentum.[28]

The spin angular momentum is determined by the number of unpaired electrons in the 3d orbital. The number of unpaired electrons for Mn(II) complexes is five, since it forms high-spin d^5 complexes due to the high electron pairing energy of manganese in the 3d-orbital.[29] Only a few low-spin Mn(II) complexes are known and often need special ligands. Therefore these, are of no interest to this research.[30]

The second factor influencing the effective magnetic moment is the orbital angular momentum. This factor depends on the possibility for electrons in the 3d-orbital to change their position from orbital to orbital without inducing an increase or decrease of energy. Since Mn(II) is a high-spin d^5 complex, there is no possibility for this movement of electrons, which results in the orbital angular momentum to be 'quenched'. Therefore the contribution of the orbital angular momentum to the effective magnetic moment can be neglected .[28] It should be noted that for other oxidation states of manganese the orbital angular momentum cannot be neglected as it does affect the effective magnetic moment, see *figure 2*.[29]

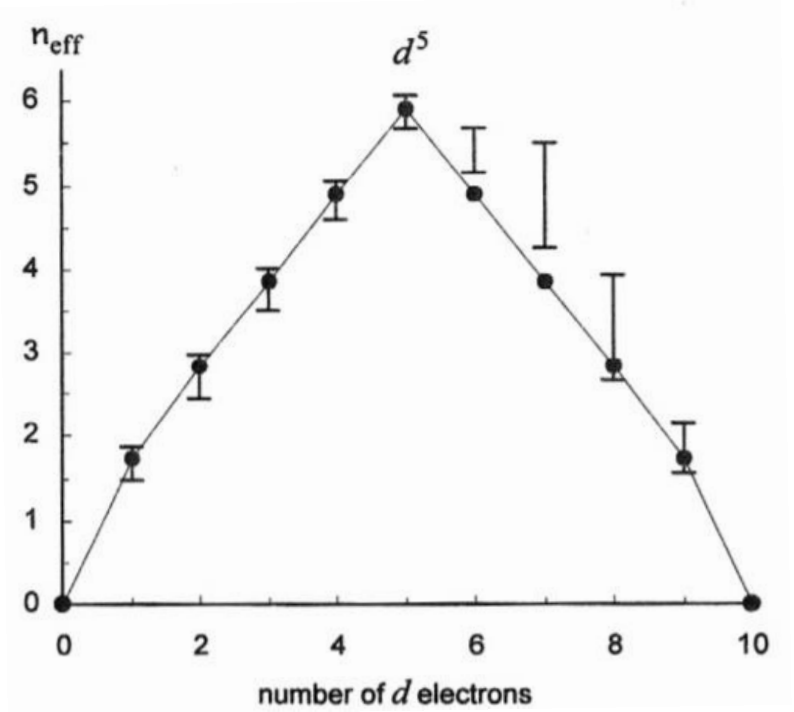

Figure 2: The orbital angular moment results in deviations from the spin only formula, see eq.3., for the first row transition metals high-spin complexes. The y-axis represents μ_{eff} and the x-axis represents the number of electrons in the 3d orbital. The black dots represent the values of the spin only formula. The beams represent the deviation due to the orbital angular momentum. The significance of the deviation is dependent on the number of electrons in the 3d orbital. For d^1 to d^4 lower values are expected compared to the spin only formula. For d^6 to d^9 higher values are expected. d^5, to which Mn(II) belongs, has a quenched orbital angular momentum. Therefore the deviation of the spin only formula is neglectable.[31]

Since the orbital angular momentum can be neglected for Mn(II) high-spin complexes, the effective magnetic moment Mn(II) can be approached with *eq. 3* based on the spin angular momentum described by J. Lewis *et al*.[32]

$$\mu_{eff} = \sqrt{n(n+2)}\ \mu_B \quad (3)$$

Where μ_B stands for Bohr Magneton, the physical constant in which μ_{eff} is expressed and n stands for the number of unpaired electrons in the complex.

Next to the spin and orbital angular momentum, ligands coordinated to the metal-centre can also influence the μ_{eff} in Mn(II) complexes to a lesser extent. There are three ways for a ligand to create a chemical bond with a metal-centre: ion dipole bonds, ionic bonds and electron pair bonds. Only the formation of an electron pair bond results in a lower μ_{eff} than would be expected according to *eq. 3.* This has only been observed for Mn(II) cyanide complexes and since cyanide will not be a ligand of interest, it has no direct impact on this research.[28]

Oxidation state of manganese and stability in manganese complexes

As seen in the previous section the effective magnetic moment of manganese depends on the number of unpaired electrons in the 3d orbital, which is determined by the oxidation state of manganese. Therefore, an understanding of the stability of the oxidation state of Mn(II) in aqueous solution is required to ascertain its effective magnetic moment.

The most commonly known oxidation states of manganese are +2, +3, +4, +6 and +7. For determination of the Mn concentration via BMS method, it should be assured that there is only one oxidation state in the solution or that the equilibrium of the oxidation states is known. Some recent findings demonstrate that the Mn(II) oxidation state acts stable in aqueous solution and no stabilizing ligands are needed.[33] Mn(III) is less stable and converts to Mn(II) and Mn(IV) over time. Mn(VI) and Mn(VII) are unstable and strong oxidizing agents.[34] Thus, when the concentrations of the oxidation states of manganese other than Mn(II) have to be determined with BMS, it is required that these oxidation states will be stabilized with an appropriate ligand to assure the correct effective magnetic moment.

ICP-OES

ICP-OES is a commonly used technique to analyse low concentrations of metals in solutions within an error range of 5%. For this reason ICP-OES will be used as reference for determining the accuracy of the new measurement method based on the BMS measured with NMR. Some general factors that are known to influence the accuracy, should be considered when analysing the results.

The presence of H_2SO_4 in the samples can result in interference with the spectrum because sulphur emits radiation in the same wavelength range as metals.[35] Additionally, very high HCl concentrations lead to down drift of the ICP-OES signal.[36] Therefore, HNO_3 is utilized to acidify the samples to assure proper ionization of the plasma.

The second factor is the concentration range at which the ICP-OES can operate. The radiation that an element emits is only linear in a specific concentration range. If the concentration of the samples becomes too high, the intensity of the radiation that the ICP-OES measures becomes 'saturated'. The ICP-OES will then measure a value that will deviate from the 'true' value of the sample. The linear emission-concentration range of a metal can be determined by developing a calibration line with accurately known concentrations.[35]

3. Materials and Methods

Chemicals

Manganese(II)chloride ($MnCl_2$), 1,4,7,10-tetraazacyclododecane-1,4,7,10-tetraacetic acid (DOTA), *tert*-butyl alcohol (*t*-BuOH), 3-(trimethylsilyl)propionic-2,2,3,3 – d4 acid sodium salt (TMSP), acetone, nitric acid 37% (w/w), deuterium oxide 99.9 atom % D and sodium hydroxide were bought from Sigma Aldrich, (Zwijndrecht, the Netherlands). Manganese ICP standard was bought from Merck, (Darmstadt, Germany) Gd-DOTP (Gadolinium(III)-1, 4, 7, 10-tetra-azacyclododecane-N,N',N“,N”'-tetrakismethylenephosphonic acid) was used from the stock of chemicals synthesized in the group earlier. MQ water was generated with a MQ machine.

Instruments

An Agilent 400-MR DD2 NMR with a 5 mm ONE NMR Probe was used for recording NMR spectra. The spectra were recorded at an ambient probe temperature of 25 °C, with a common ^1H proton spin at a bandwidth of 399.7 MHz. An internal deuterium lock was used (4.8 ppm). The analysis of the peaks was performed with MestReNova™ software.

Inductively coupled plasma – optical emission spectrometry (ICP-OES) was conducted with a OPTIMA 4300DV Perkin Elmer ICP-OES (Perkin Elmer, Waltham, MA USA) under the following operating conditions: RF power 1350 W, nebulizer gas flow 0.8 L/min, auxiliary gas flow 0.2 L/min sample, Sample Flow Rate 1.50 mL/min. The detection wavelengths: 342.246, 336.225, 335.048 and 308.199 nm were selected for the quantification of Gd. The detection wavelengths: 257.61, 259.372, 260.568, 294.92, 293.305, 279.482 and 403.075 nm were selected for the quantification of Mn.

NMR and ICP-OES sample preparation and measurement

All NMR samples for BMS measurements were prepared with different concentrations of Mn(II) containing compounds in a solution of 1% *t*-BuOH in MQ water (0.5 mL) in a 5-mm NMR outer tube and a solution of 1% *t*-BuOH in D_2O (0.1 mL) in a 4-mm NMR inner tube, unless noted otherwise.

All samples for ICP-OES measurements were prepared out of the same concentrations of Mn(II) containing compounds used for the NMR samples. All the samples were diluted in 2 mL HNO_3 37%(w/w) and a specific quantity of MQ water was added to every solution to assure that every sample was diluted to a concentration that lay within the range of the calibration line of 1.0 – 10.0 mg/L Mn(II).

The calibrations for ICP-OES measurements with Mn(II) were performed with four concentrations: 0.9657 mg/L, 5.0850 mg/L, 7.3799 mg/L and 9.9045 mg/L Mn(II), unless noted otherwise. The calibrations for ICP-

OES measurements for Gd(III) were performed with four concentrations: 2.0444 mg/L, 8.1249 mg/L, 14.1100 mg/L and 20.0829 mg/L Gd(III). Both the Mn(II) and Gd(III) concentrations were prepared out of a 1000 mg/L stock solution.

NMR and ICP-OES measurements: Gd-DOTP

NMR and ICP-OES measurements were performed, according to the procedure in section *'NMR and ICP-OES sample preparation and measurement',* with five different dilutions of Gd-DOTP stock solution. The solutions for Gd-DOTP were prepared by diluting the stock solution resulting in the following concentrations of Gd(III): 9.8, 4.9, 2.6, 1.0 and 0.1 mM.

Synthesis of Mn-DOTA

The Mn-DOTA complex was synthesized according to a method published in the literature.[15] $MnCl_2 \cdot 4H_2O$ (54.1 mg, 0.273 mmol, 1.0 eq.) was dissolved in MQ water (5 mL) and DOTA (116 mg, 0.286 mmol, 1.05 eq.) was added to this solution. The mixture was stirred for one hour on a magnetic plate stirrer after which the pH was measured being at 3.1. The pH was brought back to 6.5 by slowly adding a solution of 1 M NaOH. Directly after the synthesis, the solution was clear. After a couple of days brown precipitation was observed. The Mn-DOTA was kept in solution to be used for ICP-OES and NMR measurements.

NMR and ICP-OES measurements: Mn-DOTA and $MnCl_2$

NMR and ICP-OES measurements were performed, according to the procedure in section *'NMR and ICP-OES sample preparation and measurement',* with six different dilutions of Mn-DOTA stock solution. The solutions for Mn-DOTA were prepared by diluting the stock solution resulting in the following concentrations of Mn(II): 14.6, 10.6, 5.0, 2.3, 1.2 and 0.5 mM.

NMR and ICP-OES measurements were performed, according to the procedure in section *'NMR and ICP-OES sample preparation and measurement',* with six different dilutions of $MnCl_2$ stock solution. The solutions for $MnCl_2$ were prepared by diluting the stock solution, which resulted in the following concentrations of Mn(II): 9.3, 4.7, 2.4, 1.0, 0.7 and 0.4 mM.

NMR BMS accuracy determination

NMR measurements were performed in triplicate, according to the procedure in section *'NMR and ICP-OES sample preparation and measurement',* with seven different dilutions of Mn(II) 1000 mg/L. The solutions were

prepared by diluting the stock solution, which resulted in the following concentrations Mn(II): 0.2736, 0.4494, 0.9382, 2.0573, 3.8557, 9.1081 and 18.2023 mM.

Oxidation measurements closed $MnCl_2$ NMR tube

Three NMR measurements were performed, according to the procedure in *'NMR and ICP-OES sample preparation and measurement',* over the course of two weeks with one dilution of $MnCl_2$ stock solution. The solution was prepared by diluting the stock solution, which resulted in the concentration of 8.6 mM.

Comparison of *t*-BuOH and TMSP as reference materials

Due to the formation of double *t*-BuOH peaks in NMR spectra of low Mn(II) concentrations it was decided to compare two reference materials: *t*-BuOH and TMSP.

t-BuOH NMR measurements were performed, according to the procedure in section *'NMR and ICP-OES sample preparation and measurement'*, with one dilution of $MnCl_2$ stock solution. The solution was prepared by diluting the stock solution, which resulted in the concentration of 0.2 mM.

TMSP NMR measurements were performed with the same concentration of 0.2 mM Mn(II) as used for the *t*-BuOH measurement. The NMR samples for TMSP BMS measurements were prepared in a solution of 1%(w/w) TMSP in MQ water (0.5 ml) in a 5-mm NMR outer tube and a solution of 1%(w/w) TMSP in D_2O in a 4-mm NMR inner tube.

4. Results and Discussions

Proof of principle: BMS and ICP-OES measurements on Gd-DOTP

D. Corsi *et al.* showed that determining the concentration of lanthanide complexes via BMS is a straightforward and accurate method. The purpose of this research is to develop a comparable method based on BMS to determine the concentration of Mn(II) complexes. The BMS method is based on the principle of determining the peak difference on an NMR spectrum between two chemically identical reference materials, except that one reference material is influenced by a paramagnetic substance and the other is not. This NMR spectrum is recorded with only one measurement using an 'outer tube' and an 'inner tube', see *figure 3.* The inner tube does not contain the paramagnetic substance, but the outer tube does. This results in the observed peak difference on the spectra which is linear to the concentration of the paramagnetic substance.

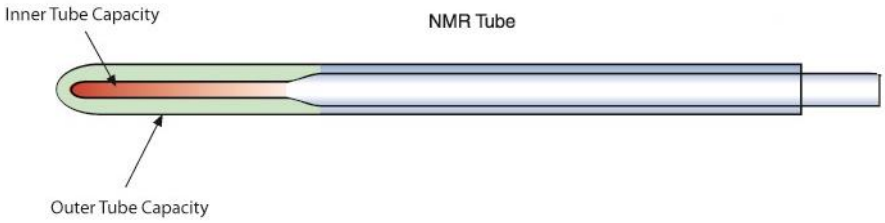

Figure 3: An illustration of an inner and outer NMR tube for performing Mn(II) and Gd(III) BMS measurements.[37]

To acquire an in-depth understanding of the experimental method of BMS and ICP-OES, a proof of principle experiment with Gd-DOTP was conducted to confirm the proposed experimental method.

A set of five pre-synthesized Gd-DOTP solutions, see *figure 4,* were prepared and measurements on the solutions were performed with NMR and ICP-OES. In this way the results could be compared, and conclusions could be drawn about the accuracy of the adapted experimental method.

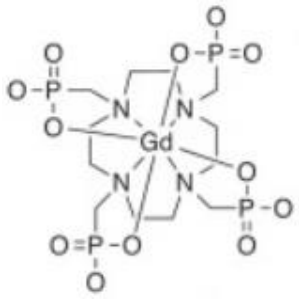

Figure 4.: The chemical structure of Gd-DOTP. Gd-DOTP was utilized for the proof of principle experiment for BMS and ICP-OES.[38]

For the NMR measurements *t*-BuOH was selected as a reference material due to its inert properties. Therefore, coupling of the *t*-BuOH to the metal ion resulting in peak splitting or hyperfine paramagnetic shifts

that would influence the accuracy of BMS determination, will be prevented. Additionally, decrease of partial molar volumes of water and *t*-BuOH when dissolving *t*-BuOH in water, can also be neglected.[39]

In *figure 5,* the NMR spectra of measurements performed on the Gd-DOTP concentrations are presented. The concentrations based on BMS, ICP-OES and Gravimetric analysis are shown in *table 1*. The concentrations lay in a range from 0.67 mM to 6.63 mM and increase from (A) to (D) which results in an increase in shift between *t*-BuOH in the inner tube and *t*-BuOH in the outer tube. The lowest concentration of Gd-DOTP that was measured is demonstrated in *figure 6*. At this concentration level it was difficult to accurately determine the BMS. Therefore, the minimum concentration threshold for which NMR is still a feasible method to determine the BMS induced by Gd(III) is 0.045 mM.

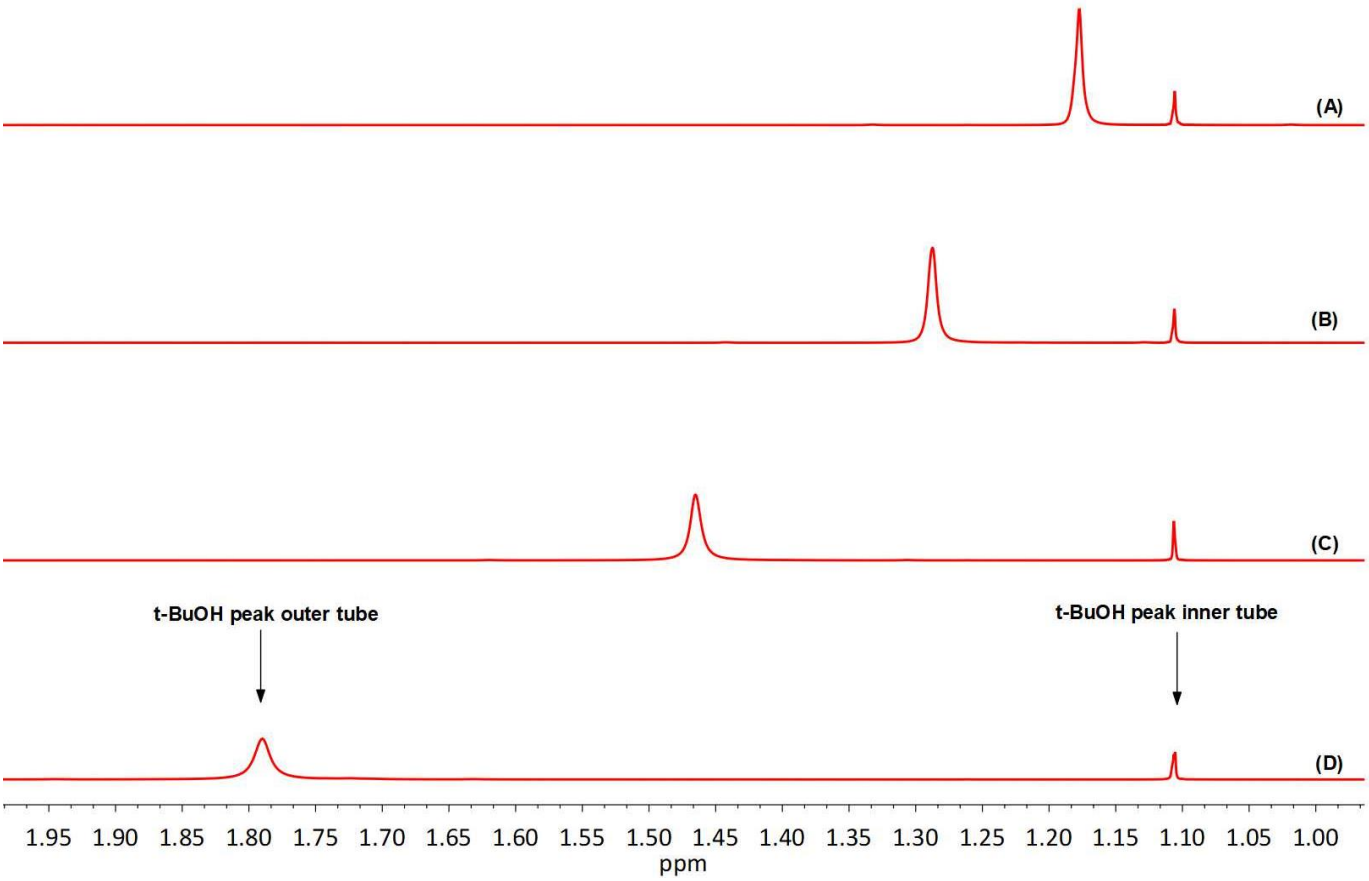

*Figure 5: The BMS induced by paramagnetic Gd(III) in the outer tube solution is demonstrated. The peak on the right side of the spectrum at 1.1067 ppm, is the t-BuOH peak in the inner tube without Gd(III). The concentration of Gd(III) in the outer tube increases from **(A)** to **(D)** resulting in an increase in shift between t-BuOH in the inner and outer tube.*

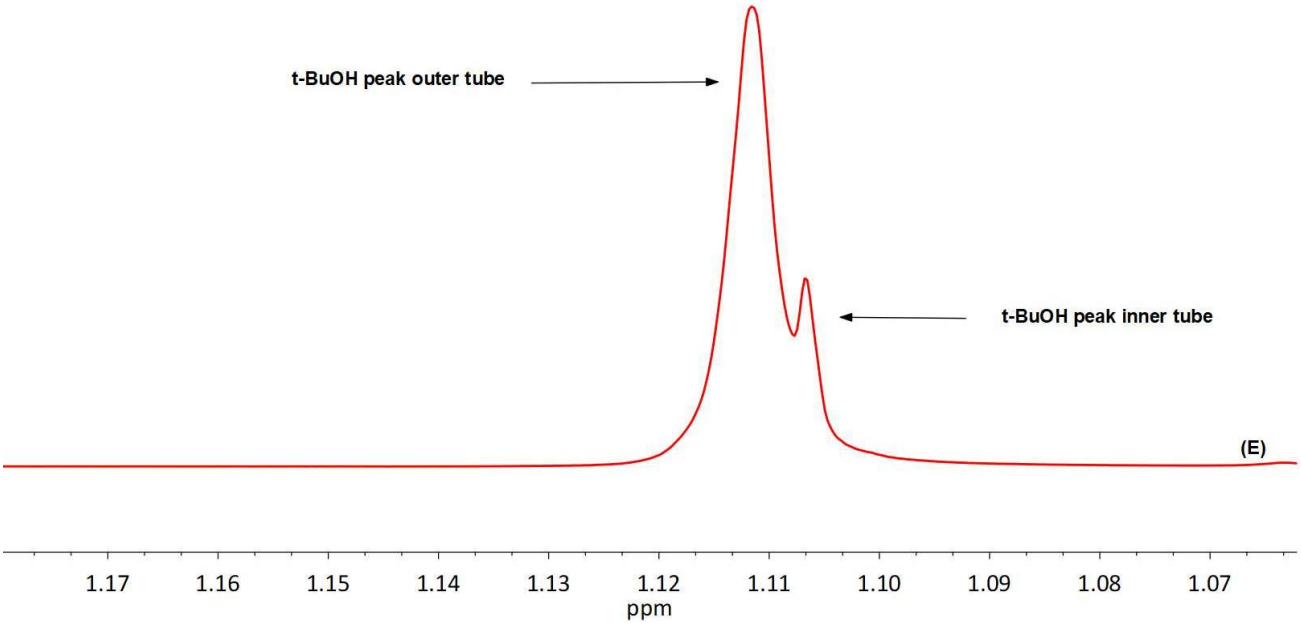

Figure 6: The BMS induced by Gd(III) at a concentration of 0.045 mM. At this concentration, the inner and outer tube peaks start to interfere with each other, making it difficult to determine the BMS.

ICP-OES measurements were performed with the same concentrations. The values of BMS and ICP-OES align within a margin of 1%. Only for the highest concentration (6.63 mM Gd(III)) a difference of 5% is found, since this sample had to be diluted multiple times to reach a measurable concentration. Something that was applied in a lesser extend to the other samples.

The significantly higher concentrations determined by gravimetric analysis can be explained by the fact that the Gd-DOTP consisted of impurities that were not removed during the synthesis process. Examples of impurities could be Cl^-, the counter-ion of Gd(III), or Na(I), the counter-ion of NaOH during synthesis.

Gd-DOTP Solution	Δx (ppm)	Concentration Gd(III) (mM)			Difference BMS relative to ICP (%)
		BMS[a]	ICP-OES	Gravimetric	
A	0.0716	0.6684	0.6650	0.9812	0.51
B	0.1813	1.6673	1.7292	2.5585	-3.58
C	0.3587	3.2988	3.3343	4.9333	-1.06
D	0.6835	6.2859	6.6320	9.8123	-5.48

Table 1: The Gd(III) concentrations obtained from BMS, ICP-OES and gravimetric analysis. [a]The BMS and ICP-OES concentrations are in agreement. The concentrations of the gravimetric analysis deviate from BMS and ICP-OES due to impurities in the synthesized Gd-DOTP. BMS calculations were performed with eq. 2.

The results compare well with the results presented by D. Corsi *et al.*[23] and our results even show a smaller difference in percentage between ICP-OES and BMS concentrations compared to literature.

In conclusion, the experimental method adapted has proven to be accurately in determining the concentration of Gd(III) with BMS as well as ICP-OES.

Synthesis of Mn-DOTA

Since the proposed method for measuring Gd(III) concentrations via BMS was successful, the method was applied to determine Mn(II) in solution as a free ion as well as Mn-DOTA. Mn-DOTA complex was used, since it has proven to be very stable in aqueous solution.[15]

The synthesis of Mn-DOTA was performed by adding DOTA and $MnCl_2$ in water and stirring the solution for an hour, see *figure 7.* The molar ratio DOTA : $MnCl_2$ was 1.05 : 1.00 to assure that all the Mn(II) would be incorporated in the DOTA ligand. $MnCl_2$ was chosen since Cl^- is known to be a relatively inert counter-ion in the synthesis of metal-complexes and does not affect the oxidation state of Mn(II). The latter is of great importance for the BMS measurements. To compare the inertness of Cl^- as counter-ion, SO_4^{2-} was utilized for the synthesis of Mn-DOTA, since SO_4^{2-} is known to be less chemically inert than Cl^-.[40] Both complexes were analysed with BMS and ICP-OES. BMS and ICP-OES analysis performed with Cl^- were in better agreement than analysis performed with SO_4^{2-}, proving the chemical inertness of Cl^-.

After the synthesis of Mn-DOTA, a pH of 3.1 was measured, which was adjusted to 6.5 using NaOH, to precipitate the remaining Mn(II) as $Mn(OH)_2$. A decrease of pH was expected during complex formation of DOTA with Mn(II), because of the carboxyl groups from DOTA repelling there H^+ ion to coordinate to the Mn(II).

NMR spectra of Mn-DOTA showed a weaker peak broadening effect compared to free Mn(II) at the same concentration. This weaker relaxing effect aligns with our expectations since Mn(II) has a coordination number of six. Therefore, there is no possibility for a water molecule to coordinate to Mn-DOTA in the inner sphere, which reduces the relaxation enhancement effect. In comparison, free Mn(II) in solution can coordinate six water molecules in the inner sphere, resulting in a much stronger relaxation effect. Therefore, these NMR spectra confirm that Mn-DOTA has been synthesized.

After a couple of days, brown precipitation was formed in the Mn-DOTA solution. This could be explained by the fact that $Mn(OH)_2$, which could be present in the solution, was oxidized to MnO_2 due to exposure to air.[33]

In conclusion, Mn-DOTA has been synthesized, which was confirmed by a decrease in relaxation effect for the Mn-DOTA solution compared to the free Mn(II) solution. A decrease of pH after the synthesis also indicates complex formation between Mn(II) and DOTA. On the foundation of these results, the Mn-DOTA solution was used for ICP-OES and BMS measurements to investigate the feasibility of the BMS method.

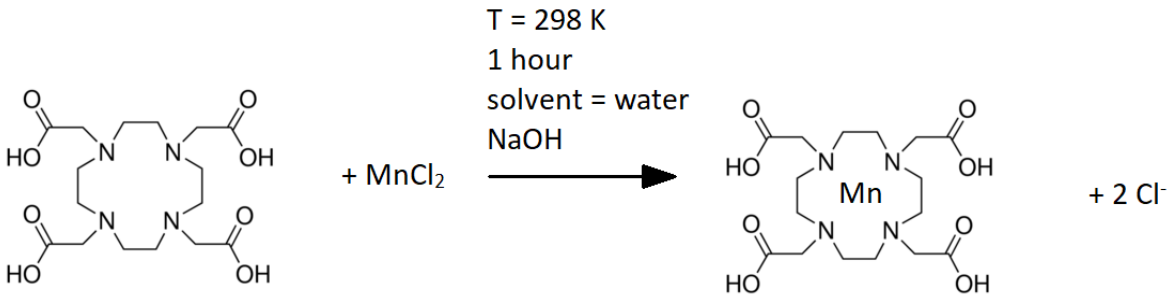

Figure 7: The synthesis of Mn-DOTA.

BMS and ICP-OES measurements: Mn-DOTA and $MnCl_2$

To determine the feasibility of the BMS method, the concentrations obtained from BMS and ICP-OES, were compared. The analysis was performed with samples in a concentration range from 0.2 mM – 15.1 mM, since this is the concentration range of interest for investigating potential Mn(II) CAs.[41] Measurements were performed with Mn-DOTA complex and with free Mn(II), for which Cl^- was chosen as a counter-ion due to its inert properties.

The results of the BMS and ICP-OES measurements on Mn-DOTA and $MnCl_2$ are presented in *table 2* and the results of the recorded NMR spectra for BMS in *figure 8.* The concentrations obtained from BMS are in well agreement with those measured by ICP-OES for Mn-DOTA as well as for free Mn(II) ($MnCl_2$,) although two deviations from the expected results could be observed.

$MnCl_2$ Solution	Δx (ppm)	Concentration Mn(II) (mM)		Difference BMS relative to ICP (%)
		BMS[a]	ICP-OES	
E	0.0263	0.4351	0.4336	0.35
F	0.0434	0.7180	0.6785	5.82
G	0.0577	0.9546	0.9019	5.84
H	0.1428	2.3624	2.2186	6.48
I	0.2771	4.5843	4.2693	7.37
J	0.5289	8.7500	8.5916	1.80
Mn-DOTA solution				
K	0.0327	0.5500	0.5393	1.98
L	0.0726	1.2011	1.1842	1.43
M	0.1423	2.3542	2.3208	1.44
N	0.3032	5.0160	4.9556	1.22
O	0.6823	11.2878	10.5561	6.93
P	0.9139	15.1192	14.6035	3.53

Table 2: The concentrations of Mn(II) as a result of BMS and ICP-OES measurements for $MnCl_2$ and Mn-DOTA. [a]The BMS and ICP-OES concentrations are in agreement. BMS calculations were performed with eq. 2.

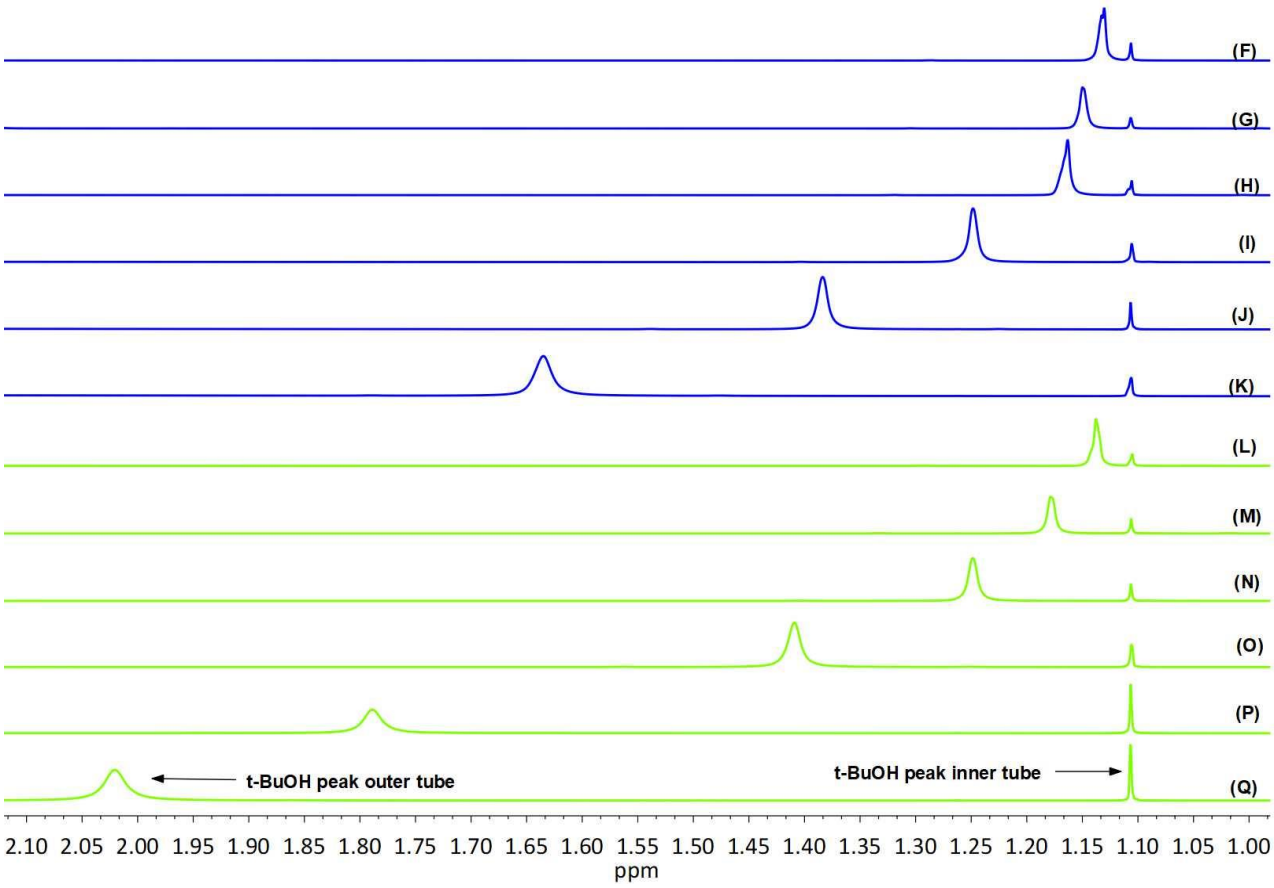

*Figure 8: The BMS induced by free Mn(II) ($MnCl_2$) in the outer tube solution is shown for **(F)** to **(K)** and by Mn-DOTA for **(L)** to **(Q)**. The peak on 1.1067 ppm is the t-BuOH peak in the inner tube without Mn(II). The concentration of Mn(II) in the outer tube increases from **(L)** to **(Q)** and from **(F)** to **(K)** resulting in a lager peak difference between inner and outer tube.*

The first deviation is the tendency of the BMS method to consistently measure a 1-5% higher concentration for all samples compared to ICP-OES for both Mn-DOTA and $MnCl_2$. This could be the result of two factors.

(1) One possibility is that during sample preparation for the BMS measurements the solvent was evaporated, resulting in a concentration higher than the actual one. Although this upward deviation was not noticed with BMS measurements performed on Gd-DOTP.

(2) The second possibility is the adaption of the wrong effective magnetic moment for Mn(II). A higher actual effective magnetic moment would explain the higher BMS than expected. In literature there are cases stating deviations from the effective magnetic moment of 5.92 for Mn(II) complexes, but no specific values are given for Mn-DOTA and $MnCl_2$ (*Section 2. Background: effective magnetic moment).*

The second observed deviation is the larger relative difference between $MnCl_2$ concentrations measured with BMS and ICP-OES (1-2%), than for Mn-DOTA concentrations measured with BMS and ICP-OES (5-7%). This could be the result of four factors.

(1) One factor is the previously mentioned possibility of solvent evaporation. The $MnCl_2$ and Mn-DOTA BMS measurements have been conducted via the same method, but within different time frames, which could have resulted in more solvent evaporation for $MnCl_2$ solutions than for Mn-DOTA solutions.

(2) The second factor is a different average oxidation state (AOS) for free Mn(II) compared to Mn-DOTA. There is a possibility that the used solid $MnCl_2$ contained traces of $MnCl_3$. This Mn(III) could have been stabilized during complex formation with DOTA, resulting in Mn(III) being present in the solution for the long term. The Mn(III) could have reduced to Mn(II) over time in the samples with free Mn(II).[34] Therefore, the AOS for the free Mn(II) solutions would have been lower compared to the Mn-DOTA solutions, resulting in a higher average effective moment and higher BMS for free Mn(II).

The experiment focused on investigating the stability of the AOS of free Mn(II) samples. Therefore three BMS measurements over two weeks were performed on a closed NMR tube with a $MnCl_2$ solution, see *figure 9.* As conclusion, the BMS did not change and thus the AOS of free Mn(II) samples is stable over time and does not affect the average effective magnetic moment.

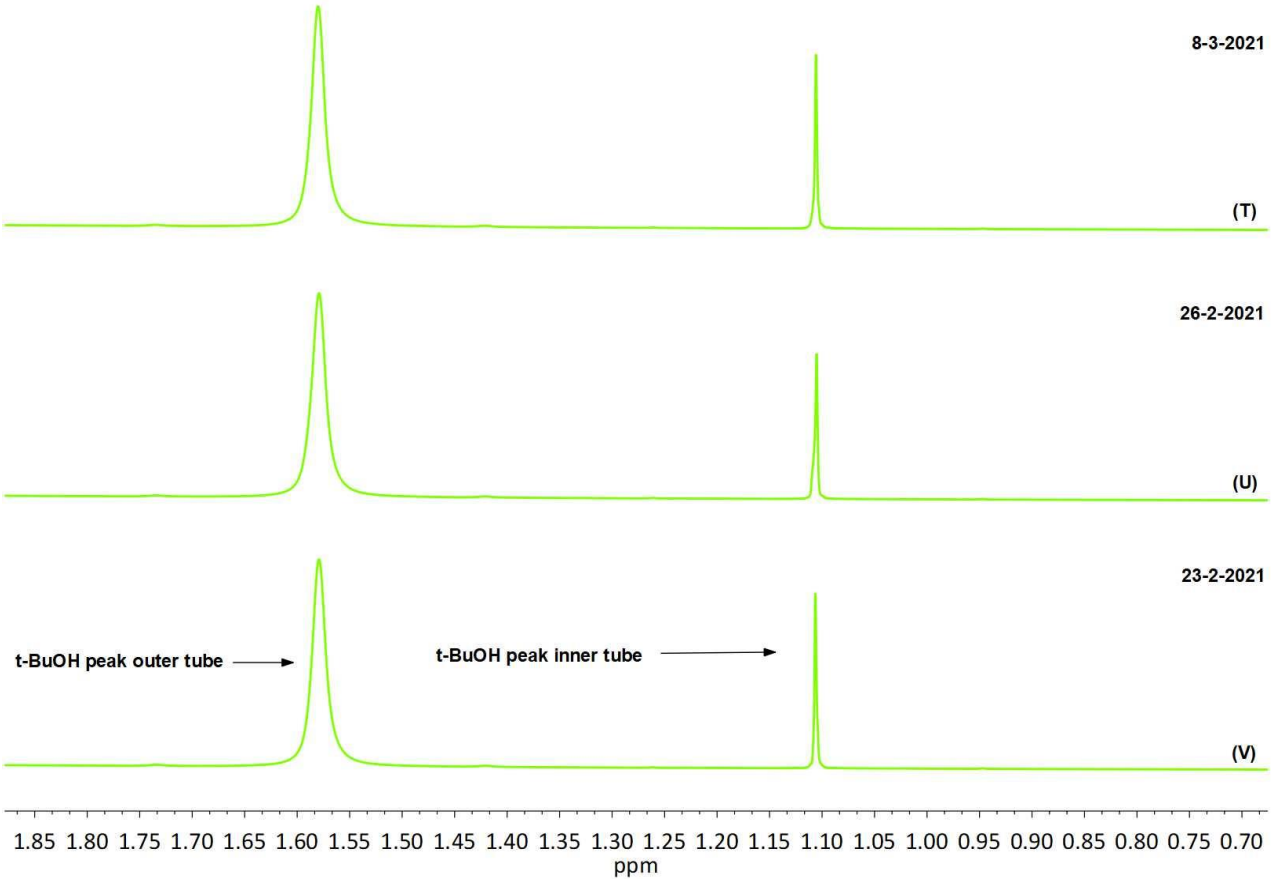

Figure 9: The BMS induced by paramagnetic Mn(II) in the outer tube is demonstrated. The peak at 1.1067 ppm is the t-BuOH peak in the inner tube without Mn(II). The concentration of Mn(II) in the outer tube is constant from day 0 ***(V)*** *until day 14* ***(T).*** *However, the measurements were performed on different dates over two weeks. The BMS does not change over time and it could be therefore concluded that the AOS of free Mn(II) is stable in aqueous solution.*

(3) The third possible factor is that the hyperfine shift, which was assumed neglectable, did have a significant impact on the observed BMS, in literature cases of a significant hyperfine shift are mentioned.[42] The hyperfine shift could be different for free Mn(II) compared to Mn-DOTA, because *t*-BuOH would have different coupling pathways to free Mn(II) compared to Mn-DOTA, resulting in a different BMS. This possible phenomenon was investigated, in which two measurements were performed with a NMR sample containing a concentration of 4 mM Mn(II). The first measurement was without DOTA. For the second measurement

DOTA was added and after complex formation an NMR spectrum was recorded. The results are shown in *figure 10.* No change in BMS was observed, thus the hyperfine shift does not affect the BMS of free Mn(II) and Mn-DOTA.

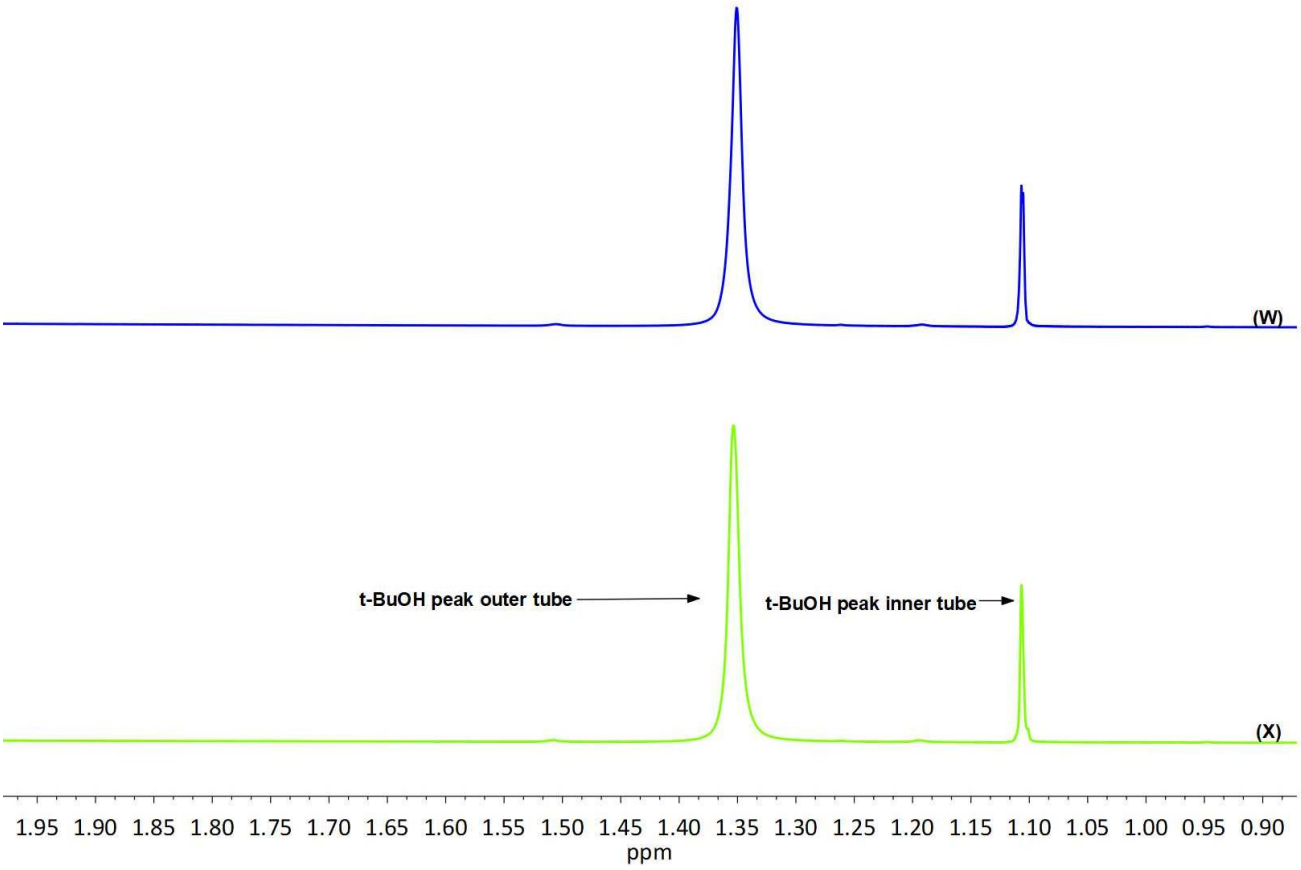

Figure 10: NMR spectra before and after addition of DOTA are demonstrated. ***(W)*** *represents the BMS induced by 4 mM of free Mn(II) and* ***(X)*** *represents the BMS after addition of DOTA to the same tube. There is no difference in BMS observed.*

(4) The fourth factor that could have induced the relative higher difference between ICP-OES and BMS measurements for $MnCl_2$ than for Mn-DOTA is a measurement error from the ICP-OES. The measurements for $MnCl_2$ and Mn-DOTA with ICP-OES were not performed in the same matrix. The difference between the two matrixes was the adapted calibration line, since the calibration of Mn-DOTA had an extra calibration point of 0.9657 mg/L Mn(II). This could have resulted in a larger measurement error for $MnCl_2$ than for Mn-DOTA.

In conclusion, the BMS method for measuring Mn(II) concentrations are in agreement with ICP-OES. There are two important anomalies that require further research. (1) Firstly, the BMS method consistently measures a higher concentration than the ICP-OES method. This deviation was not noticed for the measurements performed with Gd-DOTP. (2) Secondly, the relative higher concentration difference between BMS and ICP-OES for $MnCl_2$ compared to Mn-DOTA. This could possibly be attributed to calibration deviations in ICP-OES between the two measurements.

NMR BMS accuracy determination

Since the BMS method for measuring Mn(II) concentrations has proved to be successful, the accuracy of this new method was determined. To achieve this goal, three variables had to be investigated.

First, the random error which is caused by unpredictable and unknown changes inherent to the experiment. This error indicates the 'preciseness' of the experiment. Second, the systematic error. This error indicates the 'accuracy' of the experiment and is the deviation of the true value of an experiment.[43] Third, the lowest concentration that can be 'accurately' and 'precisely' measured with the BMS method. First, the results of the systematic and random error measurements will be discussed, followed by the lowest concentration threshold.

The random error and systematic error were determined as following. Mn(II) solutions in the range of 0.25 – 20 mM were prepared with the manganese ICP stock solution. Measurements on every concentration were performed in triplicate. The difference between these three measurements deducted the random error of the method. Furthermore, the concentrations measured with BMS were compared with the actual concentrations and the systematic error was deducted. The results are presented in *figure 11* and *figure 12.*

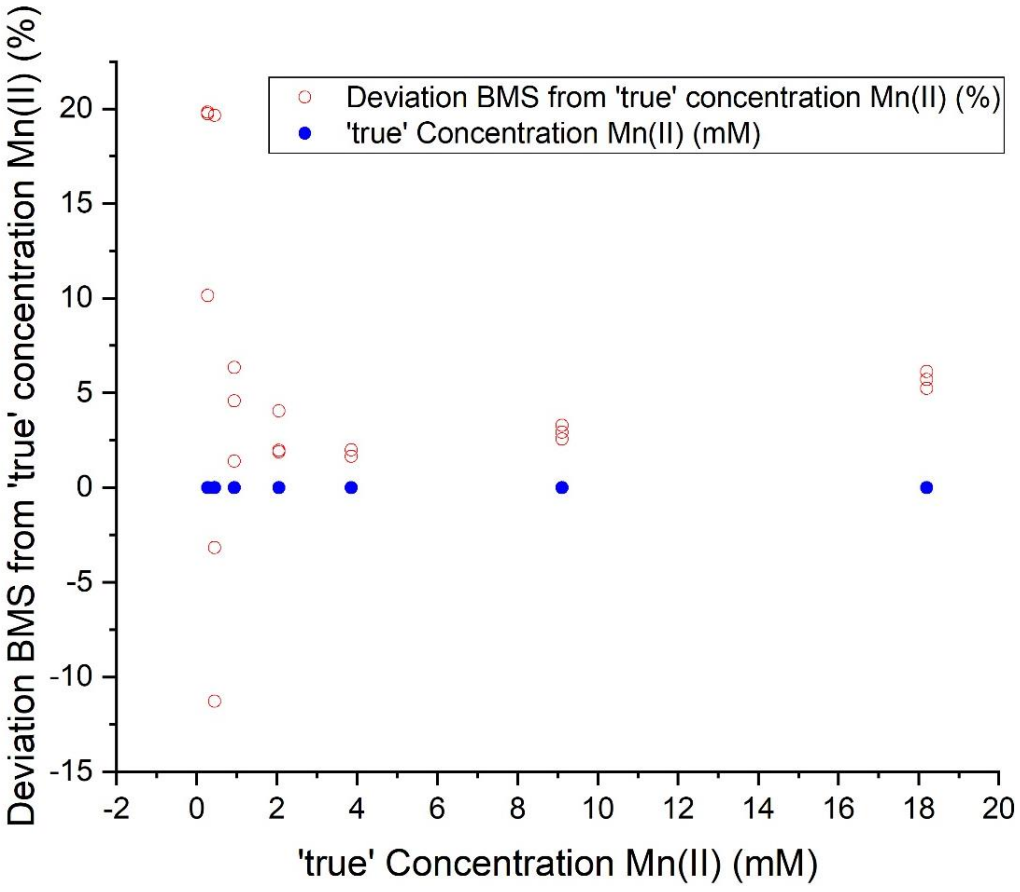

Figure 11: The relative deviation for the BMS in percentage at different concentrations is demonstrated. The red dots represent the relative deviation of the measurement from the actual concentration value which is represented by the blue dot. This difference is the systematic error. There could be observed that the relative systematic error is 2.5 % at a concentration of 4 mM and increases gradually with higher concentrations. The relative random error could be determined out of the vertical difference between the different red dots. The relative random error approaches zero from 4 mM onwards. However, for lower concentrations the random error strongly increases.

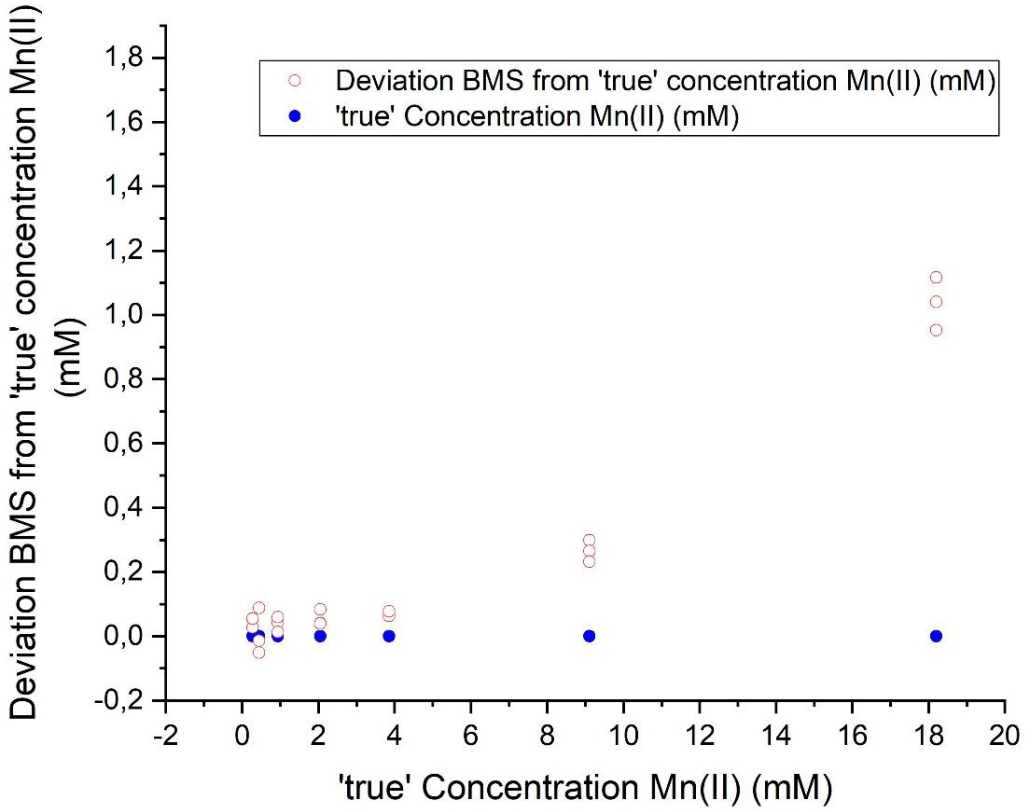

Figure 12: The absolute deviation for the BMS in mM at different concentrations is demonstrated. The red dots represent the absolute deviation of the measurement from the actual concentration value which is represented by the blue dot. This difference is the systematic error. The random error could be determined out of the vertical difference between the different red dots.

The vertical difference between the positions of the red dots represents the random error of the method. It could be concluded from *figure 11* that the random error relatively decreases with an increase of concentration. At the lowest concentrations of around 0.27 mM Mn(II), the error varies from 20% down to -12%. This represents a difference of 32% for two measurements on the same concentration which is a significant random error. This random error gradually decreases with an increase of concentration and from 4 mM Mn(II) onwards, the relative random error comes close to zero. The significant random error at low concentrations could be explained by the fact that the inherent measurement error of the NMR in determining peak position comes to lay in the same range of the Δx (ppm) BMS shift induced by the Mn(II).

The vertical difference between the blue dots and the red dots represents the systematic error. It could be concluded from *figure 11* that the systematic error is on average 2.5 %. At the lowest concentrations it is hard to determine the systematic error since the random error at this concentration level is very high. The systematic error slightly increases from 4 mM to 20 mM. This could be attributed to the fact that at high concentrations peak broadening by the relaxing effect of Mn(II) starts influencing the correct determination of the peak positions.

The systematic error that is on average 2.5 % could be attributed to two causes. (1) Firstly, this error is not being inherent to the measurement method, but an error caused by the adoption of a wrong experimental or theoretical model. This possibility is discussed in the previous section *'BMS and ICP-OES measurements on Mn-DOTA and $MnCl_2$'.* The noticed systematic error would therefore not be a 'true' systematic error. (2)

Secondly, this systematic error is inherent to the measurement method that could have resulted from a tendency of the NMR to record a slightly higher BMS than is the case.

In conclusion, the random error decreases from low to high concentrations and is close to zero from 4 mM onwards. The systematic error could be a result of the application of a wrong experimental or theoretical model. Further research is required to determine if this is the case.

In addition to the experiments that were performed for the random and systematic error, two experiments were performed to determine the lowest possible concentration of Mn(II) that could be measured in a solution with BMS.

The first experiment was set up by measuring a concentration range from 0.15 – 0.4 mM Mn(II) to determine the critical point where the BMS would lose its accuracy. This point was found at 0.20 mM Mn(II), see *figure 13*. It was observed that for both the free Mn(II) and Mn-DOTA concentrations the non-homogeneity of the peaks start at around 0.20 mM Mn(II). This phenomenon was not observed at the lowest concentration threshold for Gd-DOTP, where the peaks stayed homogenous but started to interfere with each other at lower concentrations (0.045 mM), see *figure 4*. Therefore, the peak splitting could be attributed to the interaction of Mn(II) and *t*-BuOH with each other, since this is the only different factor from the Gd-DOTP experimental set up.

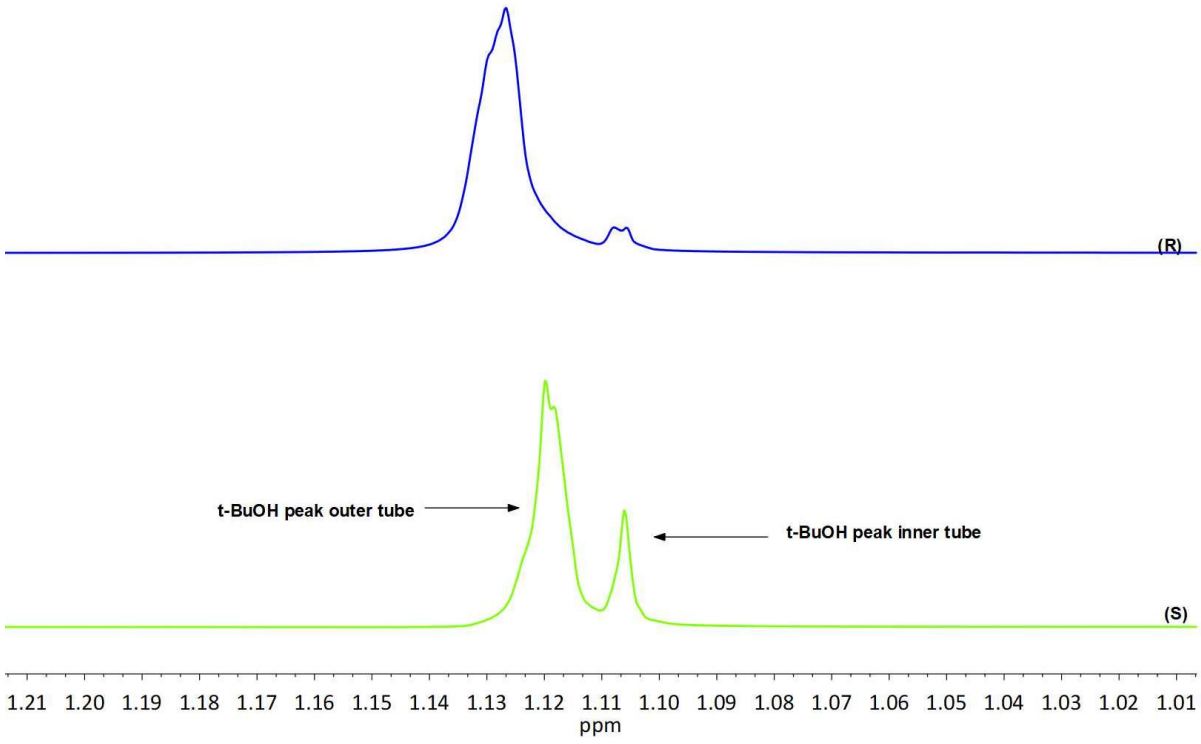

*Figure 13: The peak splitting observed for Mn-DOTA **(R)** and the peak splitting observed for free Mn(II) **(S)** at 0.20 mM. This peak splitting is the limiting factor in determining low Mn(II) concentrations with BMS.*

To investigate the possible interaction between Mn(II) and *t*-BuOH resulting in peak splitting, measurements were also performed with another reference material: TMSP, see *figure 14*. If the peak splitting would not be observed for this reference material the peak splitting could be attributed to the nature of *t*-BuOH Mn(II) interactions. Measurements were performed with a 0.20 mM Mn(II) solution using *t*-BuOH and TMSP, of which the results are presented in *figure 15* and *figure 16.*

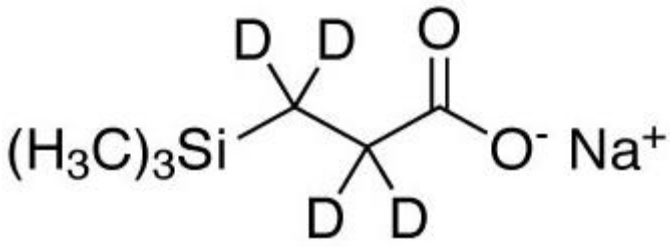

Figure 14: The chemical structure of TMSP. [44]

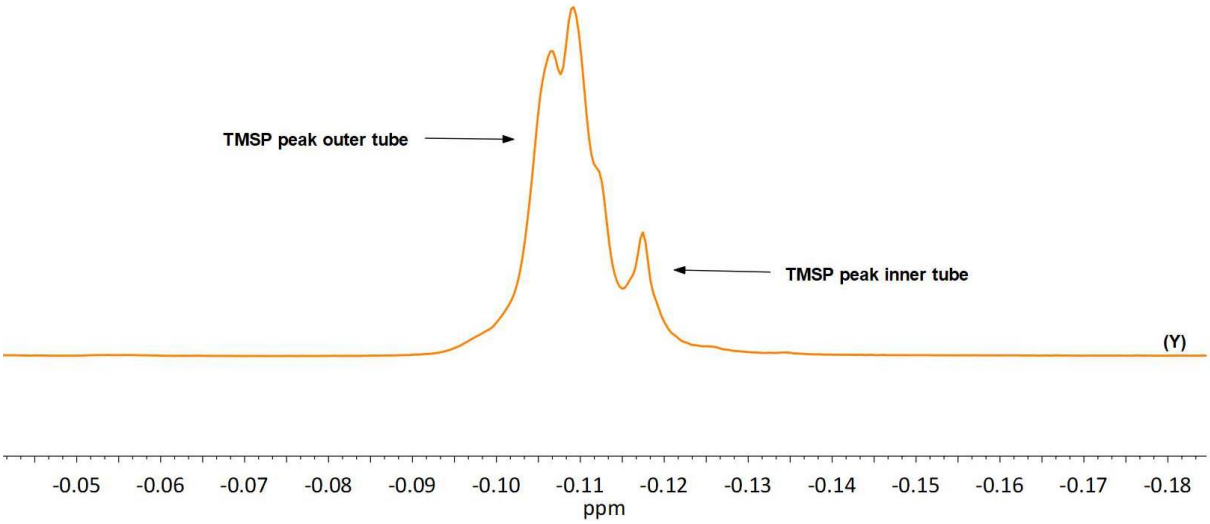

*Figure 15: The peak splitting observed for free Mn(II) at 0.20 mM **(Y)** containing TMSP as a reference material.*

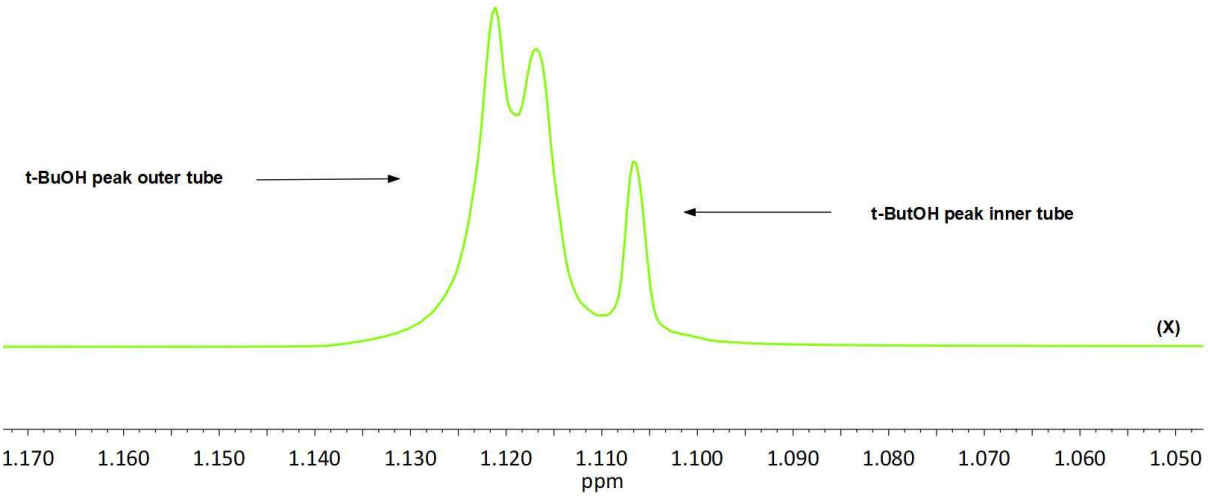

*Figure 16: The peak splitting observed for free Mn(II) at 0.20 mM **(X)** containing t-BuOH as a reference material.*

In *figure 15* it is demonstrated that with the use of TMSP as a reference material the non-homogenous peaks are also observed. It can therefore be concluded that the peak splitting at low concentrations for *t*-BuOH is

not a result of specific Mn(II) *t*-BuOH interactions, but possible by magnetic field inhomogeneity during the measurements. If better experimental conditions will not show any improvements of the spectra, further research into interaction mechanisms of Mn(II) with reference materials is needed to find the cause of this peak splitting.

In conclusion, the random error for BMS measurements with Mn(II) increases with lower concentrations. The systematic error with an average of 2.5% could be attributed to the adoption of a wrong theoretical or experimental model. More research into reference materials for BMS is required to explain the observed peak splitting for *t*-BuOH at low concentrations (0.20 mM Mn(II)).

5. Conclusions

The goal of this study was to develop a facile method for the determination of Mn(II) concentrations in NMR by adopting the similar BMS method known for lanthanides and demonstrating its reliability by verification with ICP-OES. For this purpose, several experiments were conducted.

The first experiment focussed on verifying the applied experimental method for BMS and ICP-OES measurements. ICP-OES and BMS measurements were performed with Gd-DOTP and were in good agreement within the 0.7-6.6 mM Gd(III) concentration range. Therefore, the correctness of the applied experimental method was proved. At the concentration level of 0.045 mM Gd(III) the inner and outer tube *t*-BuOH peaks started interfering with each other, making it difficult to determine the BMS.

Subsequently, BMS and ICP-OES measurements were performed with Mn(II) concentrations. The BMS and ICP-OES were in good agreement within the 0.4 – 15.1 mM Mn(II) concentration range. Nevertheless, an upward concentration deviation of 1-7% was observed for BMS compared to ICP-OES, which was not observed for Gd-DOTP measurements. This could be caused by the adoption of the wrong effective magnetic moment for Mn(II) or solvent evaporation of BMS samples. There are cases known for a deviating effective magnetic moment of Mn(II), but literature lacks the information on specific experimental situations. Hence, more research into the effective magnetic moment of Mn(II) is required.

Mn(II) concentration measurements were performed with free Mn(II) and Mn-DOTA. The BMS Mn-DOTA measurements demonstrated a better agreement with ICP-OES measurements, only showing an 1-3% upward deviation for BMS. In comparison, the free Mn(II) BMS measurements demonstrated a 2-7% upward deviation compared to ICP-OES. This deviation could be explained via four factors: (1) a different average oxidation state for free Mn(II) compared to Mn-DOTA, (2) the hyperfine shift, (3) ICP-OES calibration inaccuracies or (4) solvent evaporation. First, the AOS of a free Mn(II) solution was proven stable with three BMS measurements showing the same results over the course of two weeks. Second, measurements on the hyperfine shift were performed with comparing free Mn(II) and the same concentration of Mn(II) after complexation with DOTA, demonstrating no change in BMS. Therefore, the deviation between free Mn(II) and Mn-DOTA, could not be attributed to a difference in AOS or hyperfine shift. Third, the deviation could be caused by ICP-OES inaccuracies, since free Mn-DOTA was analysed with one extra calibration point compared to free Mn(II). Fourth, the deviation could have resulted from extra solvent evaporation of the free Mn(II) BMS samples. The experiment should be repeated to decide on the significance of these two possible causes.

The accuracy of the BMS method for Mn(II) was analysed in the concentration range from 0.25 – 20 mM free Mn(II). A significant relative random error of -12 – 20 % was observed from 0.25 mM up to 4 mM. From 4 mM up to 20 mM free Mn(II) the relative random error approached zero. The average relative systematic error was found to be 2.5 %. This error could probably be attributed to the applied experimental method. Additional to the random and systematic error, 0.20 mM Mn(II) was found to be the concentration were the BMS

becomes difficult to determine, due to inhomogeneity of the *t*-BuOH peaks. A comparison with TMSP as reference material at 0.20 mM Mn(II) was made, but the inhomogeneity of the peaks was also observed here. Therefore, this behaviour could not be attributed to Mn(II) *t*-BuOH interactions, but possibly to magnetic field inhomogeneity during the measurements.

In conclusion, the feasibility of the new method for the determination of Mn(II) concentrations via BMS has been proven for the concentration range 0.20 – 20 mM Mn(II). Nevertheless, the method does have limitations. From concentrations lower than 0.20 mM the method loses its accuracy. Additionally, further research is required to determine the cause of deviations between ICP-OES and BMS measurements and the relative systematic error of 2.5%

6. Recommendations

To get better insights into the BMS method for measuring Mn(II) concentrations, further research must be conducted. The desired goal is to obtain BMS concentrations which are in agreement with the actual concentration of the solution, with a minimal measurement error. To achieve this goal, the key is to get a more comprehensive understanding of the effective magnetic moment of Mn(II) and manganese in general, to conclude if this resulted in the deviation between BMS and ICP-OES. Literature does provide general theoretical models for the effective magnetic moment of manganese but no literature is available on the specific effective magnetic moments of different Mn(II) compounds in solution. Specifically, the significance of the orbital angular contribution of different manganese oxidation states complexed with various ligands should be investigated via BMS, since this could give concluding insights on the behavior of the effective magnetic moment from manganese complexes.

Additionally, the experiments for Mn-DOTA and free Mn(II) should be repeated completely simultaneously to rule out that experimental errors caused the observed deviation between the two species.

Nevertheless, the BMS method for Mn(II) proved to be accurate in determining concentrations for Mn-DOTA. To enhance the research into manganese CAs it is of importance to verify the BMS method for Mn(II) in complexation with other suitable ligands. With the verification of these other Mn(II) complexes the next step will be to demonstrate the feasibility of the method for Mn(II) complexes in biological systems with the presence of other chemicals that could influence the oxidation state of Mn(II) or the BMS in general. Ultimately, the method should be tested on serum containing *in vivo* injected Mn(II) based CA.

If the BMS method for Mn(II) appears to be a successful application in the research of CAs, it could be tested for other paramagnetic transition metals, like Fe(III) and Cu(II), which are also promising candidates for the use as CA.[45]

Literature

[1] Filler, A., *Nature Precedings*, **2009**.
[2] Clough, T.J., Jiang, L., Wong, K.-L.,Long, N.J., *Nature Communications*, **2019**. 10(1).
[3] Khairnar, S., More, N., Mounika, C.,Kapusetti, G., *Journal of Medical Imaging and Radiation Sciences*, **2019**. 50(4).
[4] Runge, V.M., Clanton, J.A., Lukehart, C.M., Partain, C.L.,James, A.E.J., *American Journal of Roentgenology*, **1983**. 141(6).
[5] de Haën, C., *Topics in Magnetic Resonance Imaging*, **2001**. 12(4).
[6] Lohrke, J., Frenzel, T., Endrikat, J., Alves, F.C., Grist, T.M., Law, M., Lee, J.M., Leiner, T., Li, K.-C.,Nikolaou, K., *Advances in Therapy*, **2016**. 33(1).
[7] Hao, D., Ai, T., Goerner, F., Hu, X., Runge, V.M.,Tweedle, M., *J Magn Reson Imaging*, **2012**. 36(5).
[8] Caravan, P., *Chemical Society Reviews*, **2006**. 35(6).
[9] Grobner, T., *Nephrology Dialysis Transplantation*, **2006**. 21(4).
[10] Martin, D.R., Krishnamoorthy, S.K., Kalb, B., Salman, K.N., Sharma, P., Carew, J.D., Martin, P.A., Chapman, A.B., Ray, G.L.,Larsen, C.P., *Journal of Magnetic Resonance Imaging*, **2010**. 31(2).
[11] Ramalho, J., Semelka, R.C., Ramalho, M., Nunes, R.H., Al Obaidy, M.,Castillo, M., *American Journal of Roentgenology*, **2016**. 37(7).
[12] Rogosnitzky, M.,Branch, S., *BioMetals*, **2016**. 29(3).
[13] Wahsner, J., Gale, E.M., Rodríguez-Rodríguez, A.,Caravan, P., *Chemical Reviews*, **2019**. 119(2).
[14] Drahos, B., Lukes, I.,Toth, E., *European Journal of Inorganic Chemistry*, **2012**(12).
[15] Drahoš, B., Kubíček, V., Bonnet, C.S., Hermann, P., Lukeš, I.,Tóth, É.J.D.T., *Dalton Transactions*, **2011**. 40(9).
[16] Drahoš, B., Kotek, J., Hermann, P., Lukeš, I.,Tóth, É., *Inorganic Chemistry*, **2010**. 49(7).
[17] Tromsdorf, U.I., Bigall, N.C., Kaul, M.G., Bruns, O.T., Nikolic, M.S., Mollwitz, B., Sperling, R.A., Reimer, R., Hohenberg, H., Parak, W.J., Förster, S., Beisiegel, U., Adam, G.,Weller, H., *Nano Letters*, **2007**. 7(8).
[18] Lu, J., Ma, S., Sun, J., Xia, C., Liu, C., Wang, Z., Zhao, X., Gao, F., Gong, Q., Song, B., Shuai, X., Ai, H.,Gu, Z., *Biomaterials*, **2009**. 30(15).
[19] Yang, L., Ma, L., Xin, J., Li, A., Sun, C., Wei, R., Ren, B.W., Chen, Z., Lin, H.,Gao, J., *Chemistry of Materials*, **2017**. 29(7).
[20] *DOTA*. **2021** [cited 2021 18-3-2021]; Available from: https://www.sigmaaldrich.com/catalog/product/aldrich/86734?lang=en&region=NL&cm_sp=Insite-_-caSrpResults_srpRecs_srpModel_dota-_-srpRecs3-1.
[21] *Gadopentic acid*. **2021** [cited 2021 18-3-2021]; Available from: https://www.medchemexpress.com/gadopentetic-acid.html.
[22] He, M., Hu, B., Chen, B.,Jiang, Z., *Physical Sciences Review*, **2017**. 2(1).
[23] Corsi, D.M., Platas-Iglesias, C., van Bekkum, H.,Peters, J.A., *Magnetic Resonance in Chemistry*, **2001**. 39(11).
[24] Harnden, A.C., Parker, D.,Rogers, N.J., *Coordination Chemistry Reviews*, **2019**. 383.
[25] Chu, S.C., Xu, Y., Balschi, J.A.,Springer, C.S., Jr., *Magn Reson Med*, **1990**. 13(2).
[26] Peters, J.A., Huskens, J.,Raber, D.J., *Progress in Nuclear Magnetic Resonance Spectroscopy*, **1996**. 28.
[27] Bertini, I., Luchinat, C., Parigi, G.,Ravera, E., *NMR of Paramagnetic Molecules (Second Edition)*. **2017**, Boston: Elsevier.
[28] Goldenberg, N., *Transactions of the Faraday Society*, **1940**. 36.
[29] Chandra, S.,Kumar, U., *Spectrochim Acta A Mol Biomol Spectrosc*, **2005**. 61(1-2).
[30] Ibanphylla Syiemlieh, A., Sunshine D.Kurbah, Arjune K.De, Ram A.Lala, *Journal of Molecular Structure*, **2018**. 1151.
[31] Orchard, A.F., *Magnetochemistry*. **2007**: Oxford University Press.
[32] Lewis, J.,Wilkins, R.G., *Modern coordination chemistry: principles and methods*. **1960**, New York: Interscience Publishers.
[33] Morgan, J.J., *Geochimica et Cosmochimica Acta*, **2005**. 69(1).

[34] McCleverty, J.A.,Meyer, T.J., *Comprehensive Coordination Chemistry II: from biology to nanobiology*. Vol. 5. **2003**: Elsevier Science.
[35] Olesik, J.W.J.A.C., *Analytical Chemistry*, **1991**. 63(1).
[36] Wei, L.,Guangchao, L. *Improve Analysis Precision for ICP-OES and ICP-MS for Environmental and Geological Applications*. **2015** [cited 2021 1-4-2021]; Available from: http://tools.thermofisher.com/content/sfs/brochures/WS-ICP-OES-MS-Environmental-Geological-EN.pdf.
[37] *Inner and Outer tube NMR*. **2021** [cited 2021 19-3-2021]; Available from: https://www.wilmad-labglass.com/Products/WGS-5BL/.
[38] Wu, X., Dawsey, A.C., Siriwardena-Mahanama, B.N., Allen, M.J.,Williams, T.J., *Journal of Fluorine Chemistry*, **2014**. 168.
[39] Masao, S., *Bulletin of the Chemical Society of Japan*, **1987**. 60(1).
[40] Bi, E., Bowen, I.,Devlin, J.F., *Environmental Science & Technology*, **2009**. 43(15).
[41] Pan, D., Schmieder, A.H., Wickline, S.A.,Lanza, G.M., *Tetrahedron*, **2011**. 67(44).
[42] Bryden, C.C., Reilley, C.N.,Desreux, J.F., *Analytical Chemistry*, **1981**. 53(9).
[43] Petersen, P.H., Stöckl, D., Westgard, J.O., Sandberg, S., Linnet, K.,Thienpont, L., *Clinical Chemistry and Laboratory Medicine*, **2001**. 39(7).
[44] *TMSP*. **2021** [cited 2021 29-3-2021]; Available from: https://shop.isotope.com/productdetails.aspx?itemno=DLM-48-PK.
[45] Na, H.B.,Hyeon, T., *Journal of Materials Chemistry*, **2009**. 19(35).